



Deposited via The University of Leeds.

White Rose Research Online URL for this paper:

<https://eprints.whiterose.ac.uk/id/eprint/223043/>

Version: Accepted Version

Article:

Rahman, A., Huang, H., Ai, C. et al. (2019) Fatigue performance of interface bonding between asphalt pavement layers using four-point shear test set-up. *International Journal of Fatigue*, 121. pp. 181-190. ISSN: 0142-1123

<https://doi.org/10.1016/j.ijfatigue.2018.12.018>

Reuse

This article is distributed under the terms of the Creative Commons Attribution-NonCommercial-NoDerivs (CC BY-NC-ND) licence. This licence only allows you to download this work and share it with others as long as you credit the authors, but you can't change the article in any way or use it commercially. More information and the full terms of the licence here: <https://creativecommons.org/licenses/>

Takedown

If you consider content in White Rose Research Online to be in breach of UK law, please notify us by emailing eprints@whiterose.ac.uk including the URL of the record and the reason for the withdrawal request.



ELSEVIER

Contents lists available at ScienceDirect

International Journal of Fatigue

journal homepage: www.elsevier.com

Fatigue performance of interface bonding between asphalt pavement layers using four-point shear test set-up

Ali Rahman^{a, b}, Hengwei Huang^{a, b}, Changfa Ai^{a, b, *}, Haibo Ding^{a, b}, Chunfu Xin^c, Yang Lu^{a, b}

^a School of Civil Engineering, Southwest Jiaotong University, Chengdu 610031, China

^b Highway Engineering Key Laboratory of Sichuan Province, Southwest Jiaotong University, Chengdu 610031, China

^c Department of Civil and Environmental Engineering, University of South Florida, Tampa, FL, USA

ARTICLE INFO

Keywords:

Interface

Fatigue

Shear

4-Point shear test set-up

Asphalt pavement

ABSTRACT

This paper aims to study the fatigue performance of interface bonding between asphalt pavement layers. To fulfill this objective, a four-point shear test (4PST) set-up was developed, and a series of fatigue tests were conducted on composite asphalt beam samples made up of stone mastic asphalt (SMA) and asphalt concrete (AC) mixtures. The combined effect of test temperature (3 levels), normal pressure (6 levels), loading frequency (5 levels), and shear stress (6 levels) with single tack coat type and application rate were considered for evaluation. Two interface failure criteria were successfully adopted in this study, and high correlation was relatively found between the fatigue test results and the corresponding fatigue life criteria. Findings of this study revealed that firstly, both the interface fatigue life and shear stiffness increased at all temperatures with increasing normal stress. Secondly, with increasing loading frequency, the interface fatigue life increased at each temperature. Thirdly, shear stiffness decreased with increasing shear stress for each temperature; the decrease was more pronounced at lower temperatures. Power laws were also proposed to characterize interface fatigue life at each temperature. Finally, the results of the analysis of variance (ANOVA) indicated that unlike the fatigue life, all factors had a significant effect on the shear stiffness. A multiple regression model was established successfully to predict the initial shear stiffness.

1. Introduction

Asphalt pavement is a multi-layer structure with different material properties. Its mechanical properties are not only dependent on its layers' characteristics, but also the bonding properties between layers. Insufficient interlayer bonding may result in the development of the deformation within asphalt pavement, worsening the driving conditions, increasing pavement maintenance costs, and finally, the occurrence of premature distresses such as slippage cracking, delamination, and surface top-down cracking [1–4].

Previous studies revealed that a weak bond at the interface between the surface course and binder course could lead to a reduction in the pavement life by 40% [5]. The reasons behind poor bonding are not entirely realized yet but some contributing factors are deemed exert an influence on debonding between the pavement layers [6]: type of base course material, low compaction of subgrade or subbase or base

courses, segregation in the base course, type of bitumen of the wearing course, climatic conditions during the construction, contamination of the binder course, water flow between the layers, and inadequate or excessive tack coat application.

Owing to the great importance of interface characteristics and its crucial role in the whole pavement structure performance, it has drawn the attention of many researchers worldwide in recent years. In the literature, thus far, many experimental and numerical studies on this topic can be found accordingly. Interface bonding strength testing can be evaluated whether in the field on full-scale pavements or in the laboratory on samples using different test methods [7–14]. Test methods for assessing interfacial bonding can be categorized into 11 test protocols: (1) direct shear bond test without normal stress, (2) direct shear bond test with normal stress, (3) double shear test (DST), (4) inclined shear test, (5) torque bond test, (6) *in situ* torsion bond test, (7) direct tensile bond test, (8) *in situ* tensile bond test, (9) indirect tensile bond test, (10) 3-point shear bond test, and (11) 4-point shear bond test.

* Corresponding author at: School of Civil Engineering, Southwest Jiaotong University, No. 111, 1st Northern Section, Second Ring Road, Chengdu, Sichuan 610031, China.

Email addresses: a.rahman@my.swjtu.edu.cn (A. Rahman); hwhuang@my.swjtu.edu.cn (H. Huang); cfai@swjtu.edu.cn (C. Ai); dinghaibo@my.swjtu.edu.cn (H. Ding); chunfu@mail.usf.edu (C. Xin); luyang@swjtu.edu.cn (Y. Lu)

Nonetheless, there exists a lack of intranational accord on the test method for evaluating pavement interfacial bonding [15].

It is well-documented that different parameters such as materials characteristics, interface properties, field related testing parameters, and specimen conditions affect the interface bonding performance and strength [10,16–21]. Many researchers employed numerical modeling through layered elastic or finite element methods to study the mechanical behavior of the interface in asphalt pavement layers [22–25].

A comprehensive review of the existing literature indicates that the majority of studies on the performance of interface bonding were conducted within the context of its monotonic behavior, but comparatively fewer attention has been paid to its fatigue performance. Realistically, pavements in the field and real conditions are subjected to a significant number of cyclic loads by traffic during their service life. For this reason, the static loading conditions do not simulate the real loading state in the pavement caused by the repetitive load of moving vehicles, and the characterization of the bonding behavior, therefore, would not be accurate. Nevertheless, there has been an increasing trend towards studying interface fatigue behavior in recent years.

Romanoschi and Metcalf [11] developed a testing configuration for determining the shear fatigue behavior of the interfaces. They found that there was a linear increase in permanent shear displacement (PSD) with the number of loading cycles, and for higher stresses, the rate of increase was higher. Later, Diakhate et al. [26] conducted an experimental characterization shear fatigue behavior of interfaces through laboratory tests in order to derive an interface fatigue law. They also made a first attempt to develop a model, which could closely connect shear fatigue properties to those from the direct shear test. In another study, Diakhate et al. [27] revealed that the absence of a tack coat resulted in a reduction in bonding fatigue performance. They also proposed a method that can be used to predict the conventional interface fatigue law using accelerated shear fatigue tests.

Tozzo et al. [8] successfully developed a new model incorporating all the possible stress combinations into the interface fatigue failure. Furthermore, Tozzo et al. [28] established a relationship between dynamic and monotonic results in order to predict interface failure under cyclic loading applications based on simple monotonic tests. The succeeding study revealed that there is an acceptable correlation between the interlayer shear strength (ISS) of the monotonic shear test and the fatigue test results, and interlayer bond energy is a good predictor of the shear strength of the tack coats with a strong correlation with the fatigue test results [29].

To evaluate bonding condition at the interface between asphalt surface and semirigid base, Zhang et al. [30] applied two interface treatments, one as roughening treatment and another as emulsified asphalt treatment and conducted shear fatigue tests. Their findings revealed that the horizontal shear reaction modulus and the interface bonding percentage decreased with the loading cycles, meaning that the interface bonding conditions deteriorated owing to the cyclic loading effects. Moreover, the roughening treatment had superior performance.

Taking everything into account, the investigation of the interface behavior and its influence on the performance of asphalt pavement is in the initial stages, and certainly, further efforts are required for better understanding of the fatigue behavior of the interface between asphalt layers. Having acknowledged the fact, this study aims to deal with the matter effectively through experimental investigation of interface fatigue performance in asphalt pavement.

2. Study objective and scope of work

The primary objective of this study is to evaluate the shear fatigue behavior of the interface between two halves of composite asphalt beam samples made up of SMA and AC mixtures under different testing conditions. The tests were carried out with a new developed 4-point

shear set-up which can also apply normal pressure to the specimens. The major test factors considered in this study are temperature (3 levels), normal pressure (6 levels), loading frequency (5 levels), and shear stress (6 levels). The material used as tack coat is a kind of high-performance SBS modified asphalt binder. The effect of each parameter on the interface fatigue life and shear stiffness were evaluated, and corresponding fatigue laws were established accordingly. The results acquired from the laboratory experiment were statistically analyzed to determine the significance of each factor. Finally, a multiple regression analysis was conducted to predict the initial shear stiffness.

3. Experimental program

3.1. Test device

In this study, a four-point shear test (4PST) set-up was customized and designed to evaluate interface shear bonding behavior under either monotonic or cyclic loading conditions. The original device was developed as part of the Delft research project [31] to study the anti-reflective cracking design of asphaltic overlays. In comparison to most of existing shear test equipment, this set-up has several advantages: using representative beam-shaped specimens, removing bending moment at the interface plane and imposing a pure shear load, and the efficient use of loading system capacity to apply shear force.

Owing to several difficulties with the TU Delft device such as its large size, using big specimens etc., several modifications were made to the original design in this study (Fig. 1).

The apparatus consisted of three main parts: the loading block, supports and clamps, and bottom plate and it can be positioned inside the universal testing machine (UTM) environmental chamber. The vertical shearing load is applied from the actuator of the UTM through a connection joint to I-beam shaped loading block. Two pinned supports with coupled clamps, which are attached to the loading block, transfer and divide the applied shear force to the specimen as a function of their corresponding distance to the actuator. Symmetrically, two supports with coupled clamps, which are attached to the bottom plate, role as reaction forces. Note that this arrangement of supports produces pure shear stress at the interface plane of the specimen without inducing bending moment. The sample, which is a double-layered composite asphalt material with dimensions of ($l \times h \times w$): $280 \times 70 \times 50$ mm, should be placed inside the clamps in such a way that interface set in the space between the two middle clamps (interface zone). Center-to-center distance of middle clamps is 60 mm. Owing to this configuration, it is expected that the interface starts to fail in this zone because of shear stress induced by applying repeated loading from UTM actuator.

The normal pressure, which is representing the wheel load on the road surface, is perpendicular to the interface plane and applied through a cylinder-pump set. The normal load part consists of a cylinder, a hose, a pump, load measurement system and load distribution plates. Once the specimen is placed inside the clamps, the load distribution plates are attached to both ends of the specimen. After which, the pressure is applied to the cylinder by the hydraulic pump until the extended height of the cylinder reaches to the distribution plate. The normal load applied to the specimen is monitored by a load cell with a monitoring system which is in the opposite side of the specimen.

Two linear variable differential transducers (LVDTs) were mounted on the specimen in the interface zone to measure the relative vertical shear displacement at the interface. During testing, a data acquisition system collects the data from the load cell, confining pressure transducer and LVDTs. The whole set-up can be placed in the environmental chamber of the UTM so that tests can be carried out at varying temperatures ranging from -40 to 100 °C.

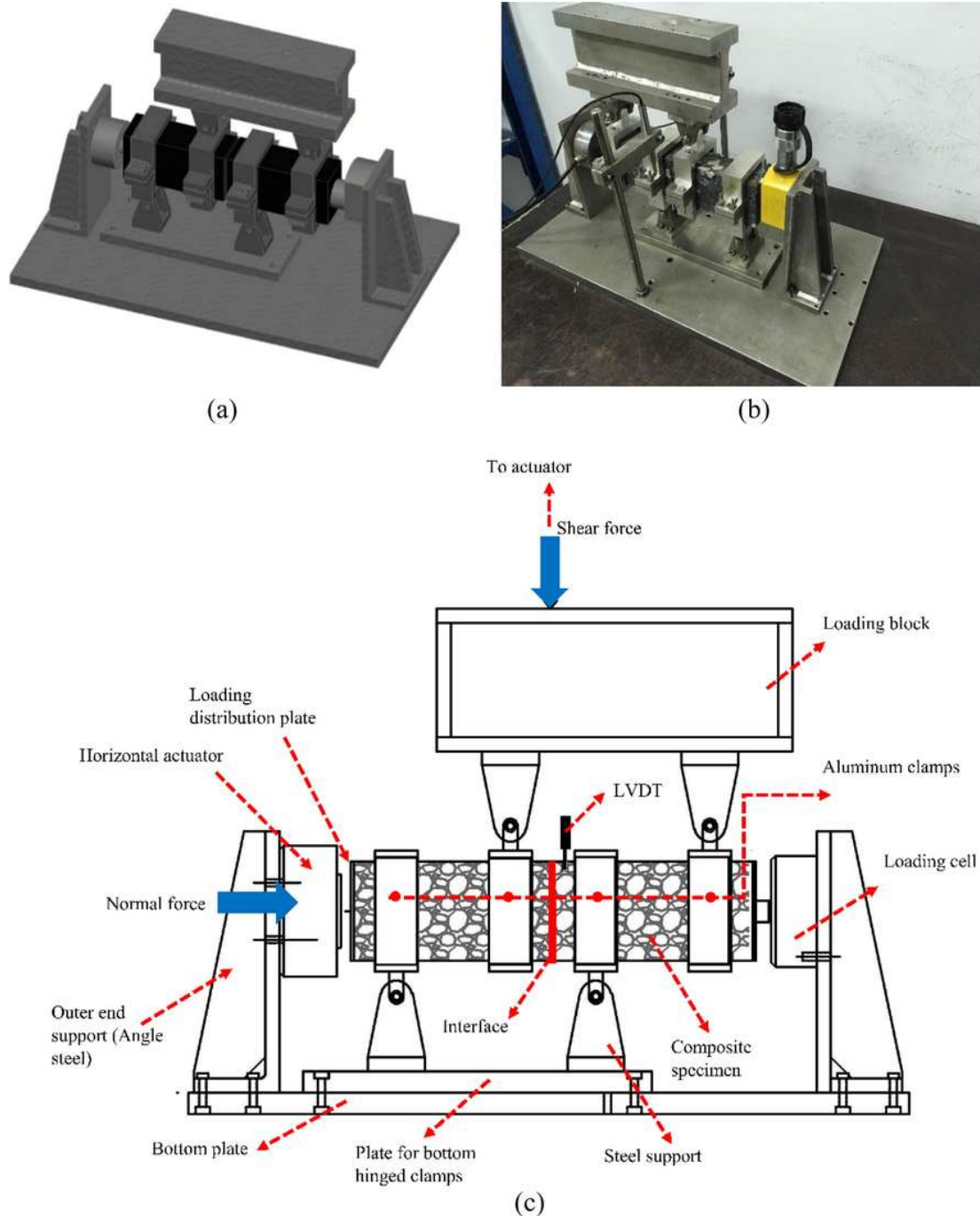


Fig. 1. 4PST set-up: (a) 3D model (b) image (c) schematic diagram.

3.2. Materials

Double-layered composite beam specimens are made up of stone mastic asphalt (SMA-13) and asphalt concrete (AC-20), which are most commonly used asphalt mixtures in the surface and binder layers of asphalt pavement respectively in China. The aggregate gradation of two mixtures is designed according to Chinese standard of JTG F40-2004 [32] as presented in the semi-log chart in Fig. 2; the type of aggregate used was limestone.

The binder type used in two mixtures was styrene-butadiene-styrene (SBS) modified asphalt with the properties shown in Table 1.

The asphalt content by weight of the total mixture was 5.8% and 4.5% for SMA-13 and AC-20, respectively.

The tack coat material selected for this study to be used at the interface was a high-performance SBS modified asphalt binder developed as part of the previous study [33]. The properties of tack coat material are shown in Table 2.

3.3. Specimen preparation

As it was mentioned in the prior section, the samples used in this study are rectangular-shaped with a cross-section dimension of 50 mm width by 70 mm height and 280 mm in length. Each beam composed of two halves representing a double-layered asphalt mixture, and an inter-

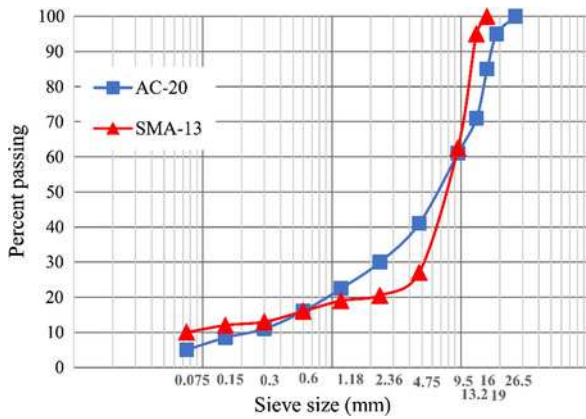


Fig. 2. Mixture design aggregate gradation.

Table 1
Properties of asphalt binder.

Property	Value	Specification limit
Penetration (100 g, 5 s, 25 °C), 0.1 mm	41.1	≥40
Ductility (cm) at 15 °C	75	≥50
Softening point (R&B) (°C)	112.1	≥85
Flash point (°C)	276	≥260
Tests on residue from thin-film oven test:		
Mass loss (%)	0.06	≤0.6
Retained penetration (%)	88.2	≥65

Table 2
Properties of tack coat material.

Property	Value	Specification limit
Softening point (R&B) (°C)	113.4	≥85
Ductility (cm) at 15 °C	68	≥50
Penetration (100 g, 5 s, 25 °C), 0.1 mm	42.8	≥40
Flexural tensile toughness (-20 °C) (kPa)	427.5	≥400
Flexural tensile modulus (-20 °C) (MPa)	96.2	≤100
Tests on residue from thin-film oven test:		
Mass loss (%)	0.02	≤0.6
Retained penetration (%)	83.1	≥65
Flash point (°C)	265	≥260

face plane in between for tack coat application. It should be noted that the production of each asphalt mixture was conducted according to the Chinese standard of JTG F40-2004 [32].

A steel mold with the plan dimensions of 300 × 400 mm and 100 mm depth was utilized to prepare asphalt mixture. First, the SMA loose mixture (160 °C) was placed in one-half of the mold and evenly distributed. Then, a roller compactor was employed to apply a certain number of passes with vibration and compact the mixture to the height of 100 mm. The target air void content of the SMA-13 mixture was set at 3.5%. After which, the compacted mixture was allowed to cool down to room temperature for 24 h before the tack coat application.

For applying the tack coat, the SBS modified asphalt binder was heated to the specified application temperature, and then, it was uniformly applied on the cleaned surface at desired application rate (0.301/m²). Subsequently, the coated surface was set aside at room temperature for 2 h to allow the curing procedure completed. Following the tack coat application and its curing, the AC-20 mixture was poured into the second half of the mold and compacted to the desired thickness (100 mm). The air void of the AC-20 mixture was designed at 5% level. The slab was left at room temperature to cool down before performing any cutting operation.

The procedure for cutting the final specimen involves several steps: procedure first, the asphalt mixture slab was demolded. Then, accord-

ing to the dimension of the final specimen, additional parts from each side of the length, width, and height of the slab was marked. Next, the additional parts were sawed and finally, from the remaining part of the slab, five test specimens were sawed and prepared for the laboratory test.

Fig. 3 illustrates the process of fabrication of specimens in the laboratory for conducting interface shear fatigue test.

3.4. Experimental parameters and test plan

To investigate the interface shear fatigue behavior of double-layered asphalt specimens, several condition variables were considered in this study: three test temperatures of 25, 35, and 45 °C; six shear stress levels of 163, 180, 196, 212, 294, and 359 kPa; six normal pressure levels of 0 (null), 28, 56, 98, 126, and 154 kPa; and five load frequencies of 1, 4, 5, 8, and 10 Hz. However, a single tack coat type and application rate (0.31/m²) were applied in this study. At each temperature, a range of 17 testing conditions was selected, and two replicates were tested for each test condition as presented in Table 3.

It should be noted that the amplitude of shear stress was chosen between 30 and 50% of the maximum shear strength of the interface obtained from the monotonic shear tests at a displacement rate of 2.54 mm/min. Combination of shear stress (τ) and normal stress (σ) was chosen in such a way that the ratio of shear to normal stress (τ/σ) is critical, i.e., where shear stress is superior to normal stress and the possibility of the interface failure is distinct owing to the passing of the wheel over the road surface [24].

The cyclic shear fatigue tests were conducted under force-controlled mode with continuous haversine waveform. A contact load of 0.1 kN was selected and maintained during testing while a maximum desired shear load was applied to induce shear fatigue failure in the specimen. Prepared samples were conditioned at the target temperature for at least 8 h before they were tested. The UTM temperature controller can adjust the temperature of the UTM environmental chamber at the desired temperature. The flow chart of the experimental program in this study is shown in Fig. 4.

4. Experimental results and discussion

4.1. Interface fatigue failure criteria

The measured applied shear force and relative displacement during the fatigue test make it possible to observe their evolution. In total, 50 data points were utilized to plot each loading/displacement cycle. The values measured for force and relative displacement during the five consecutive cycles under specific testing conditions are presented in Fig. 5.

Two main criteria were employed to identify the interface failure behavior and compare varying loading conditions. The first criterion is based on the permanent shear displacement (PSD), which was explained as the average of accumulated shear deformation obtained from two LVDTs. Fig. 6 shows the evolution of PSD with the number of load cycles at three test temperatures under similar loading conditions.

As can be seen, three distinct stages can be identified in general. At the first stage, the resistance to shear movement increases owing to position rearrangement of aggregate grains at the interface or the adjustment of the specimen up to the peak point. Then, deformation increases at a constant rate with the number of load cycles up to the point when the curve shows inflection and the interface fractures. Friction between the layers is in contact at the interface, however, will continue to hinder the relative movement. The last stage is followed by a rapid expansion of interface failure and consequently fast increase in deformation, which terminates with specimen failure. In this study, the

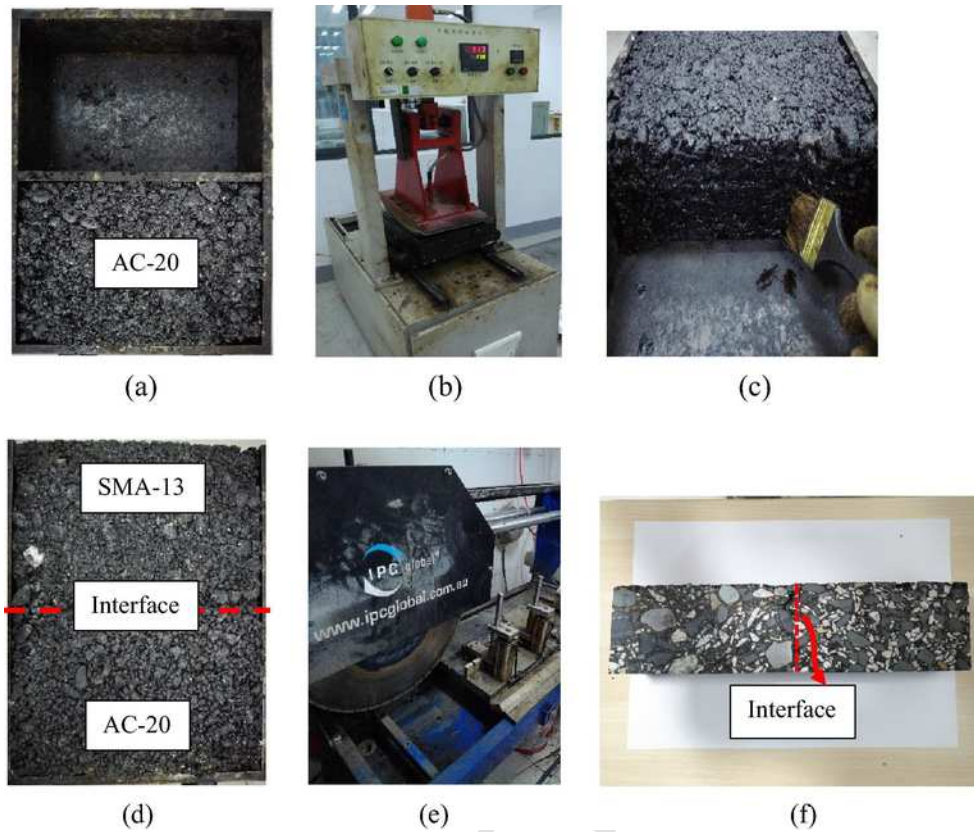


Fig. 3. The procedure of specimen fabrication: (a) Laying of AC mix (b) Compaction of the mix. (c) Tack coat application. (d) Laying of SMA mix (e) Cutting. (f) Final specimen.

Table 3
Experimental test program under each test temperature (25, 35, 45°C).

Number	Variable parameter		
	Normal pressure (kPa)	Frequency (Hz)	Shear force (kPa)
1	0	10	196
2	28	10	196
3	56	10	196
4	98	10	196
5	154	10	196
6	126	10	163
7	126	10	180
8	126	10	212
9	126	4	196
10	126	5	196
11	126	8	196
12	126	10	294
13	126	10	196
14	126	10	359
15	126	1	196
16	126	1	294
17	98	1	196

number of loading cycles that cause the detachment of the bonded layers is recorded and identified as $N_{failure}$.

As it was anticipated, at lower temperatures interface fatigue life is higher than that of at higher temperatures. The main reason lies in the fact that the tack coat is a temperature-dependent material and it is less viscous at elevated temperatures, and therefore it can easily flow at the layer interface. In fact, one may observe that as temperature increased the initial displacement amplitude at the interface raised as well. Fig. 7 depicts the specimen failure at the interface after conducting a fatigue test.

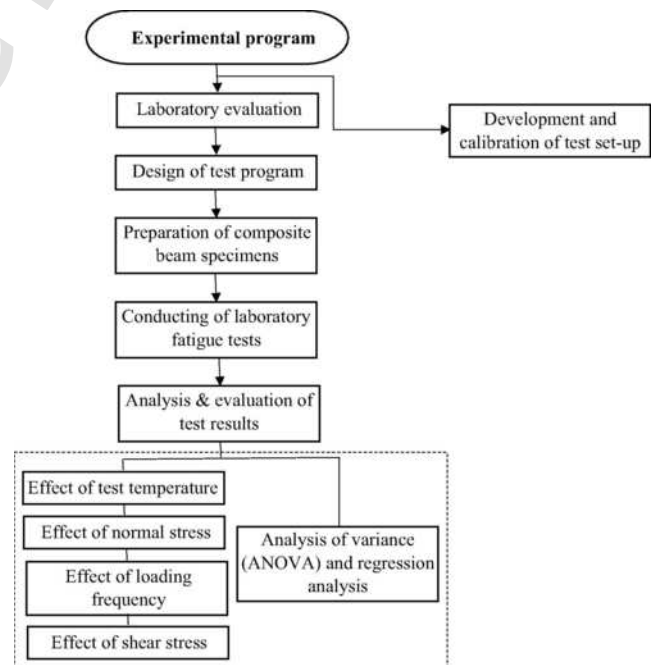


Fig. 4. Procedure of experimental program.

The second criterion is the conventional failure criterion for asphalt materials, i.e., the number of load cycles (N_{50}) when the interface shear stiffness decreases to half of its initial value (K_0). This parameter links the applied shear stress to the resulting shear slip (relative tangential displacement) at the interface. For each fatigue test, the interface shear stiffness can be denoted as a complex number $K_{s,k}^*$ as follows:

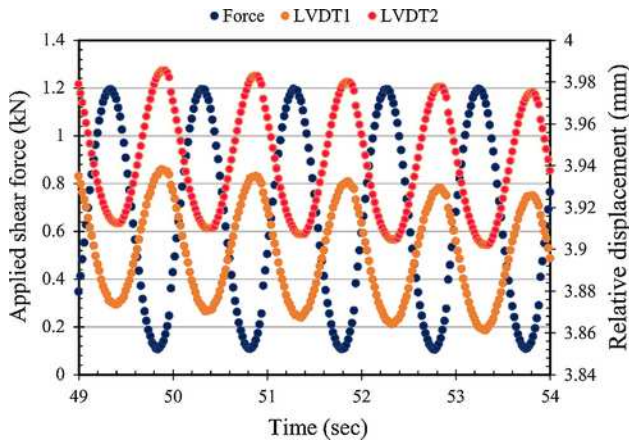


Fig. 5. Measured applied force and relative displacement during five consecutive cycles (Test conditions: 25 °C; 1 Hz; shear stress of 196 kPa; normal stress of 98 kPa).

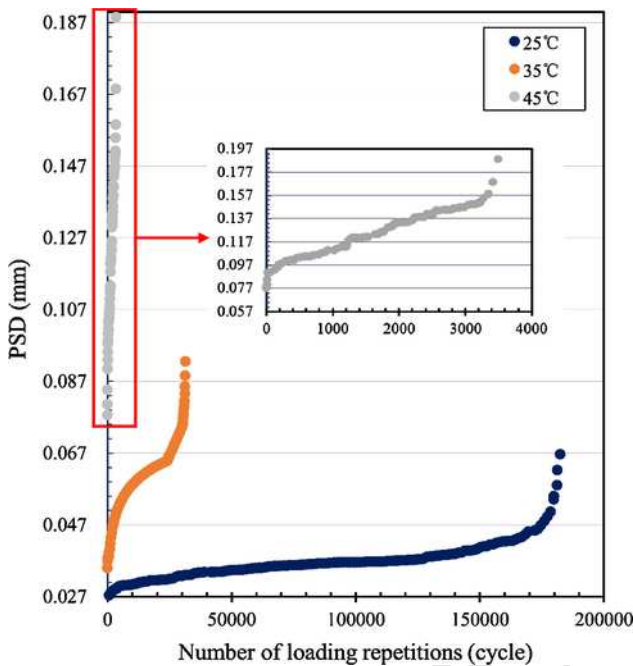


Fig. 6. PSD evolution vs. number of loading cycles at three test temperatures.



(a)



(b)

Fig. 7. Specimen failure at the interface: (a) Failed specimen (b) Two faces of the interface.

$$\begin{cases} K_{s,k}^*(i\omega) = \frac{F_k}{S \cdot u_k} \cdot e^{i\varphi_k t} & (1 - a) \\ K_{Sk} = |K_{s,k}^*(i\omega)| = \frac{F_k}{S \cdot u_k} & (1 - b) \end{cases}$$

where (at cycle #k) $K_{s,k}$ is the interface shear stiffness; F_k is the applied shear force amplitude; u_k is the amplitude of the measured relative displacement; φ_k is the phase angle between the shear force and relative displacement signals; S : sheared cross-section of interface; and $\tau = \tau_k = F_k/S$ is the amplitude of the applied shear stress.

Fig. 8 illustrates the gradual change in interface shear stiffness with increasing loading cycles at three test temperatures under similar loading conditions.

The recorded trend demonstrates three stages for each temperature. At the first stage, the modulus rapidly decreases as damage grows and microcracking occurs. Then, the stiffness is becoming a plateau at the second stage. Finally, the failure is characterized by a sharp decline of the stiffness value which means fast propagation of macroscopic cracks at the interface. In this study, the number of cycles corresponding to a 50% reduction in the initial stiffness value (N_{50}) was considered as interface fatigue life. It is evident that the shear stiffness, which is a temperature-related parameter, increases with decreasing temperature. With increasing shear stiffness, bonding between adjacent layers, and interface shear resistance will improve and finally, longer fatigue life of interface could be expected.

Fig. 9 shows the number of loading repetitions to fatigue failure (N_f) against the initial displacement amplitude for all testing conditions at three temperature levels. As can be seen, the best model that fitted the scattered data at each temperature (25, 35, and 45 °C) was power model with a high coefficient of determination (R^2) of 0.974, 0.910, and 0.936, respectively. Fig. 9 displays that the increase in initial displacement resulted in a decrease in the fatigue life at each temperature. Moreover, with increasing temperature, the resulting initial displacement increased, therefore, interface fatigue life decreased. The main reason is that the stiffness of tack coat materials at elevated temperatures decreases with increasing temperature and displacement amplitude increased as a result.

To further investigate the correlation between the initial shear stiffness (K_0) and the fatigue life acquired according to the 50% stiffness reduction method (N_{50}), K_0 was plotted against N_{50} in Fig. 10 for all test conditions at three temperatures. The relationship between K_0 and N_{50} was also plotted, and power-law expressions were fitted to examine the relationship. It is evident that there exists a high correlation between K_0 and N_{50} at three test temperatures. The higher the initial shear stiffness, the longer fatigue life is expected at each temperature.

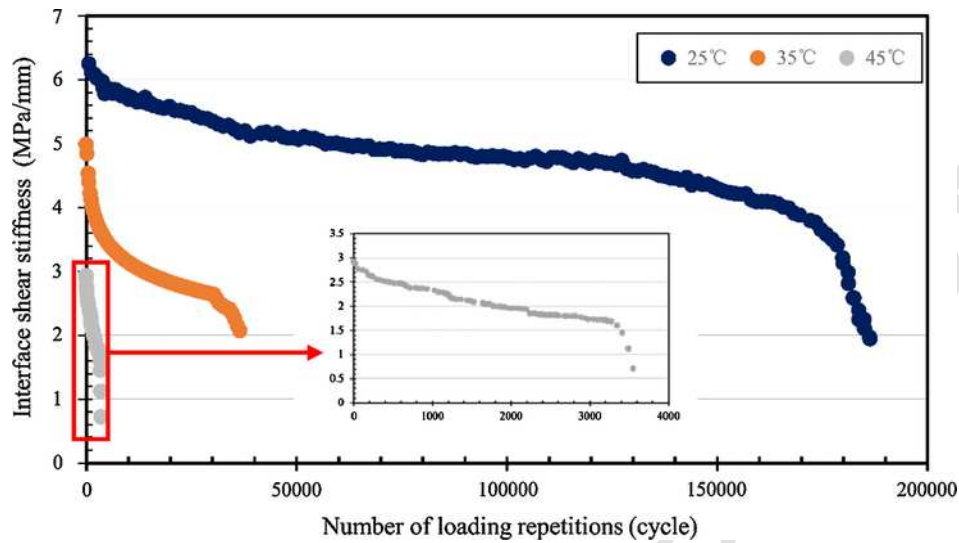


Fig. 8. Evolution of interface shear stiffness vs. the number of loading cycles at three test temperatures.

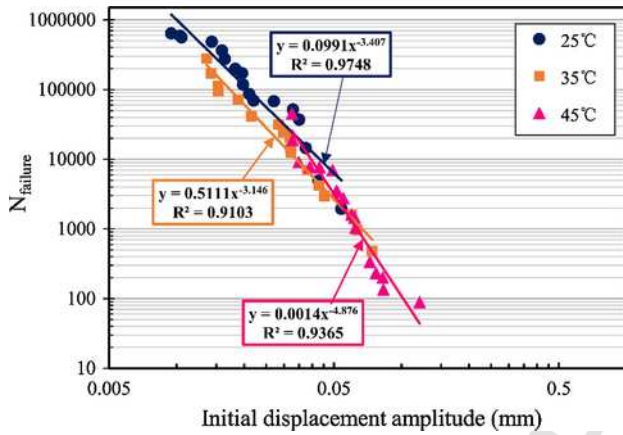


Fig. 9. N_f vs. initial displacement amplitude at $T = 25, 35,$ and 45°C .

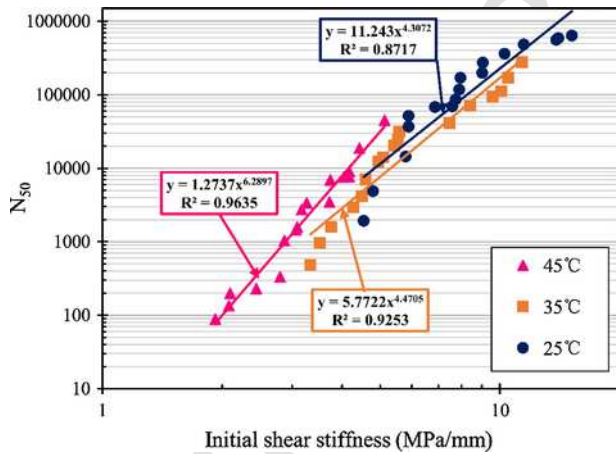


Fig. 10. N_{50} vs. initial shear stiffness at $T = 25, 35,$ and 45°C .

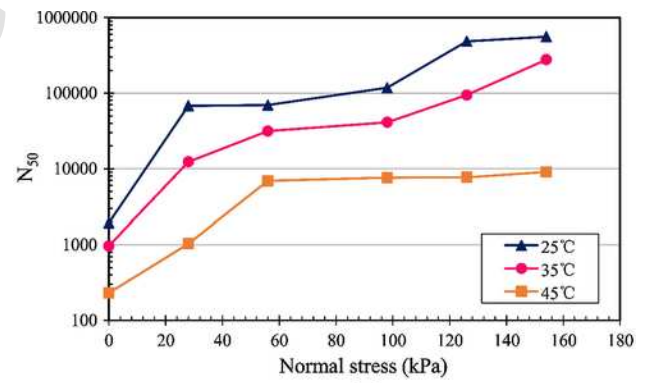
In fact, the higher initial stiffness means that the interface adhesion between two layers is strong which leads to a higher fatigue resistance of interface.

Initial evaluations, until now, showed that the developed of 4PST set-up could successfully characterize interface fatigue behavior under varying testing conditions. In the subsequent sections, a further assess-

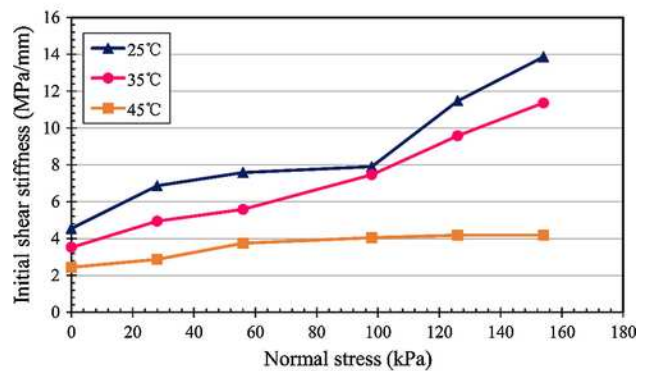
ment regarding fatigue performance of interface bonding between asphalt layers will be presented.

4.2. Effect of normal pressure

To evaluate the influence of normal pressure on the interface bonding fatigue behavior, the N_{50} and K_0 data were plotted versus the normal pressure level for each test temperatures as presented in Fig. 11. According to Fig. 11(a), it is evident that with increasing normal pressure from zero to higher values the interface fatigue life increased substantially at all temperatures. In this regard, interface fatigue life im-



(a)



(b)

Fig. 11. Normal stress level vs. (a) N_{50} (b) initial shear stiffness at $T = 25, 35,$ and 45°C .

proved by 30 times when applied normal stress reached 56kPa at 45 °C, however, further increase of normal pressure had a negligible effect on the fatigue life. One possible reason is that increasing normal pressure at high temperature can improve the friction between asphalt layers, and therefore fatigue life to a certain extent. After which further increase in normal pressure has an insignificance impact on the interface fatigue life. On the other hand, increasing normal pressure from null to 154 kPa consistently enhanced interface fatigue life by 290 and 288 times at 25 and 35 °C, respectively.

Results presented in Fig. 11(b) demonstrates that the changing trend of K_0 against normal stress level at each temperature is consistent with fatigue life results. This result indicates the linear reliance of K_0 and consequently, interface fatigue life on normal stress in shear mode. At elevated temperatures, where adhesion has minimal effect, the frictional component formed because of normal stress increases shear stiffness through prevention of aggregate movement at the interface and hence will improve fatigue life.

In summary, application of normal pressure perpendicular to interface plane, which resembles the tire contact pressure on the road surface, plays a crucial factor in the interface fatigue life, and its absence during testing would result in a conservative assessment of interface fatigue life.

4.3. Effect of loading frequency

The direct impact of the loading frequency (f) on the interface bonding fatigue life was also considered in this study. The scatter log-log diagram between the loading frequency and N_{50} was depicted in Fig. 12 for each test temperature. The best model that fitted the fatigue data acquired using 4PST set-up was the power model with relatively high R^2 values of 0.917, 0.968, and 0.966 for 25, 35, and 45 °C, respectively.

It is obvious that with increasing loading frequency, the fatigue life increased for each temperature. As it was expected with increasing temperature at each loading frequency, interface fatigue life decreased correspondingly. Moreover, the rate of increase in the fatigue life with loading frequency was linear. In this respect, the rate of improvement in fatigue life from 1 to 10Hz loading frequency under the test temperatures of 25, 35, and 45 °C were 13, 23, and 23 times, respectively. As shown in Fig. 12, the difference in fatigue life between the different temperatures was significant at higher frequencies than that of at lower frequencies.

Fig. 13 depicts the shear stiffness as a function of loading frequency and temperature. The influence of frequency on shear stiffness is evident. At high temperature (45 °C), variation in stiffness with frequency is not considerable, whereas at lower temperatures (25–35 °C), one can observe a significant change in shear stiffness.

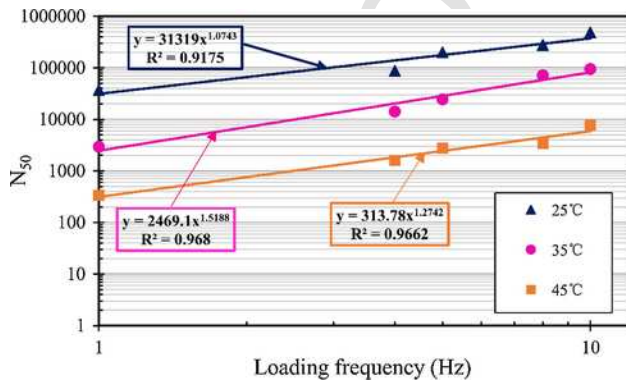


Fig. 12. Loading frequency (f) vs. N_{50} at $T = 25, 35,$ and 45°C .

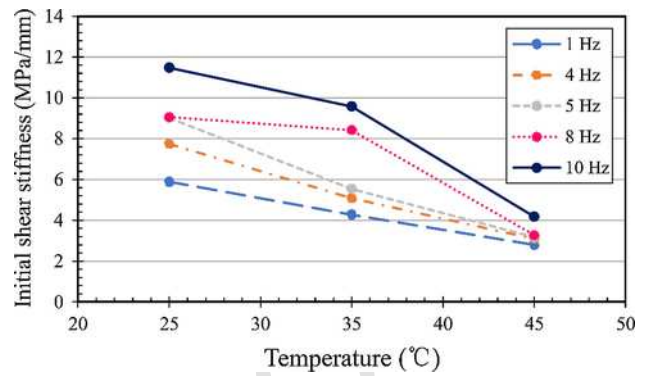


Fig. 13. Shear stiffness vs. temperature at different frequencies.

4.4. Effect of shear stress

To evaluate the influence of applied shear stress on interface fatigue behavior, the shear stress levels were plotted against the corresponding interface shear stiffness for each temperature, as presented in Fig. 14. With increasing shear stress, shear stiffness decreases for each temperature. While there is a gradual decline in shear stiffness at 45 °C, the decrease is more pronounced at lower temperatures. It is noticeable that the difference between shear stiffness of different temperatures at lower shear stress levels is more distinct than that of at higher stresses. The possible reason lies in the fact that as shear stress increases at lower temperatures, the resistance to shear movement at the interface as a result of the reduction in friction decreases. Consequently, the shear stiffness declines substantially.

Having acknowledged the significance of the interface behavior for the pavement structure performance, a bonding fatigue law to links applied shear stress with the corresponding number of cycles to failure (for 50% reduction in stiffness) is necessary. From the test results, a fatigue power law was drawn by fitting a regression line between N_{50} and applied shear stress for each temperature. The results are shown in Fig. 15.

It is evident that the estimated power laws to characterize interface fatigue behavior for each temperature are appropriately fitted with linear regression and high R^2 values. As expected, the higher shear stress, the lower fatigue performance of the interface for each temperature. The rate of decrease in the fatigue life with shear stress at elevated temperature (45 °C) was higher than that of at lower temperatures. The slope coefficients in the fatigue models clearly show this phenomenon. Compared to higher temperatures, at lower temperatures, the adhesion component between the pavement layers plays a crucial role in interface bonding fatigue life against applied shear stress. On the whole, the

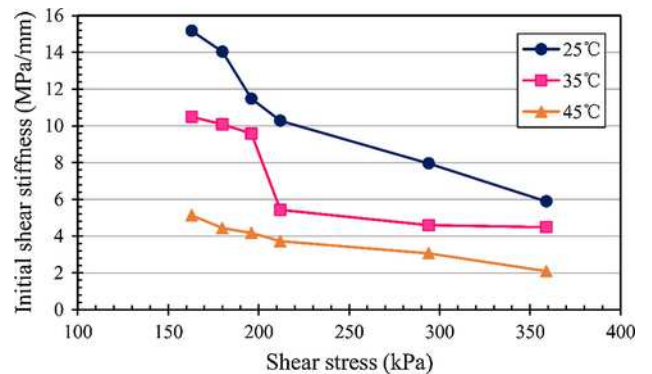


Fig. 14. Shear stiffness vs. shear stress at $T = 25, 35,$ and 45°C .

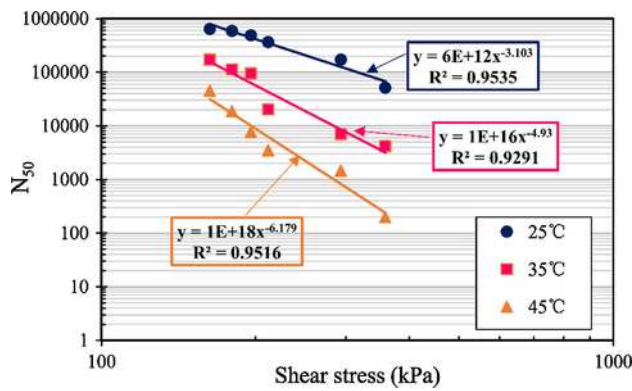


Fig. 15. Fatigue laws for T = 25, 35, and 45 °C.

effect of shear stress on the fatigue life of the interface at higher temperatures is more significant than at lower temperatures.

4.5. Analysis of variance (ANOVA) and regression analysis

Based on the above results it can be found that temperature, loading frequency, shear, and normal stresses have an influence on K_0 and N_{50} . However, the significance level of each factor remained unknown. For this reason, the statistical analysis of variance (ANOVA) was employed to determine the significance of each factor for K_0 and N_{50} statistically. The analysis was performed according to data obtained from the test program in this study. ANOVA assembles a collection of statistical procedures to quantitatively specify whether certain parameters and their combinations affect particular responses, which are K_0 and N_{50} in this study.

Table 4 ANOVA for ΔK_0 .

Factor	DF ^a	SS ^b	MS ^c	F-value ^d	P-value
Temperature	2	248.19	124.094	64.41	0.000 ^e
Normal pressure	5	77.19	15.437	8.01	0.000
Frequency	4	40.77	10.193	5.29	0.002
Shear stress	5	87.93	17.586	9.13	0.000
Error	34	65.50	1.927		
Total	50	544.51			

- a Degrees of freedom.
- b Sum of squares.
- c Mean square, which is the SS divided by DF.
- d Ratio of mean squares. It is used to determine the P-value.
- e Factor is significant (P-value < 0.05).

Table 5 ANOVA. for N_{50} .

Factor	DF	SS	MS	F-value	P-value
Temperature	2	4.26021E+11	2.13011E+11	16.72	0.000
Normal pressure	5	1.74313E+11	34862591648	2.74	0.035
Frequency	4	55186304114	13796576029	1.08	0.380
Shear stress	5	1.56312E+11	31262451057	2.45	0.053
Error	34	4.33186E+11	12740756728		
Total	50	1.31146E+12			

Table 6 Results of multiple regression for K_0 .

Coefficient										R ²
	a	b	c	d	e	f	g	h	i	
Value	6.431	-2.222	1.335	0.3886	-0.746	-0.552	0.495	-3.894	-0.483	0.9413

The P-value is the minimum level of significance at which the factor is deemed significant in influencing the response. In this study, the P-value of 0.05, i.e., a confidence level of 95% was considered. Tables 4 and 5 shows the ANOVA results for K_0 and N_{50} , respectively.

As shown in Table 4, P-values of all factors are all less than the significant level of 0.05. In other words, all studied factors have significant effect on the initial shear stiffness. The F-value of each factor demonstrates that the significant effect of each factor on K_0 in order of importance ranks as temperature, shear stress, normal pressure, and loading frequency. It should be noted that interface shear stiffness is closely related to the applied tack coat material which is considered as a viscoelastic material. The findings show that the stiffness of the interface is not only dependent on loading rate and temperature but also other factors like shear and normal stresses.

Table 5 indicates that the temperature and normal pressure are the only significant factors. Moreover, P-values of loading frequency and shear stress are both higher than the significance level, which implies that they have no significant effect on the interface fatigue life. Although loading frequency and shear stress according to ANOVA have no significant impact on fatigue life, their essential role in the fatigue performance of the interface cannot be neglected. In this regard, further investigation will be conducted to verify these findings.

Owing to the fact that fatigue tests are cumbersome and time-consuming, the prediction of the interface fatigue life is a matter of concern among researchers. To overcome this difficulty, a multiple nonlinear regression model was developed to analyze the changing law of initial shear stiffness. The goal is to model the variation of a quantitative response variable Y in connection with the variation of four explanatory variables. This model can be expressed as shown in the following equation:

$$Y = a + bX_1 + cX_2 + dX_3^2 + eX_1 \cdot X_2 + fX_1 \cdot X_3 + gX_1 \cdot X_4 + hX_2 \cdot X_4 + iX_3 \cdot X_4 \quad (2)$$

where Y is the initial shear stiffness; a, b, c, d, e, f, g, h, and i are regression coefficients; X_1 is the temperature; X_2 is the normal pressure; X_3 is loading frequency; and X_4 is the shear stress. The regression coefficients can be obtained by the least square method. The results of the regression analysis are presented in Table 6.

As shown in Table 6, The regression analysis demonstrates that the regression model can explain 94.13% of the variation in Y. Consequently, this equation can be used to predict the initial shear stiffness at the beginning of the test as a function of the studied factors. Note that the regression model should only be used to predict K_0 for values of the X variables that fall within the range of the X variables presented in this study.

5. Conclusions

This study mainly evaluated the fatigue performance of the interface bonding between asphalt pavement layers using four-point shear set-up. Given the results presented in this paper, the following conclusions can be drawn:

- (1) Two interface failure criteria were successfully adopted in this study. One was based on the permanent shear displacement (PSD);

the other was based on the conventional 50% reduction in stiffness. It appeared that at lower temperatures interface fatigue life was higher than that of at higher temperatures. On the other hand, the shear stiffness increased with decreasing temperature. Moreover, the best models that correlate the fatigue life with K_0 and initial displacement amplitude were established for each test temperature with relatively high R^2 values.

- (2) The interface fatigue life increased substantially at all temperatures with increasing normal stress, but further increase of normal pressure had negligible influence on the fatigue life. Similarly, the changing trend of K_0 against normal stress level at each temperature was consistent with fatigue life results.
- (3) With increasing loading frequency, the fatigue life increased at each temperature. As it was expected with increasing temperature at each loading frequency, interface fatigue life decreased correspondingly. At high temperature (45 °C), variation in stiffness with frequency is not considerable; however, at lower temperatures (25–35 °C), one can observe a significant change in shear stiffness.
- (4) Shear stiffness decreased with increasing shear stress for each temperature; the decrease was more significant at lower temperatures. Furthermore, power fatigue laws with a high coefficient of determination were also estimated to correlate interface fatigue life with shear stress for each temperature.
- (5) ANOVA results indicated that unlike the fatigue life, all factors had a significant effect on the shear stiffness. Finally, the resulting multiple regression model had an R^2 value of 0.9413 which means that the model fits the data well and the equation can be used to predict initial shear stiffness for specific values of the variables. The model presented can be considered as the first step toward prediction of conventional interface fatigue life under different loading conditions.

On the whole, the results presented in this study demonstrates that the new four-point shear set-up successfully evaluated the interface fatigue performance in shear mode and could have promising results in future applications. Nonetheless, more laboratory experiments should be conducted to verify these results. Moreover, in this study, only a single tack coat type and application rate was employed. Hence, future studies should consider different tack coat types and application rates in order to gain a deeper understanding of interface fatigue behavior.

Conflict of interest

The authors declare that they have no conflict of interest.

Acknowledgments

This work was supported by the National Natural Science Foundation of China [grant number 51878574]; and the National 973 Program [grant number 2013CB036204].

References

- [1] L.N. Mohammad, A. Bae, M.A. Elseifi, J.W. Button, J.A. Scherocman, Interface shear strength characteristics of emulsified tack coats, *J Assoc Asphalt Paving Technol* 78 (2009) 249–278.
- [2] A. Vaitkus, D. Zilioniene, S. Paulauskaite, F. Tuminiene, L. Ziliute, Research and assessment of asphalt layers bonding, *Baltic J Road Bridge Eng* 6 (2011).
- [3] M. Ling, X. Luo, Y. Chen, F. Gu, R.L. Lytton, Mechanistic-empirical models for top-down cracking initiation of asphalt pavements, *Int J Pavement Eng* (2018) 1–10.
- [4] M. Alae, Y. Zhao, S. Zarei, G. Fu, D. Cao, Effects of layer interface conditions on top-down fatigue cracking of asphalt pavements, *Int J Pavement Eng* (2018) 1–9.
- [5] K. Khweir, D. Fordyce, Influence of layer bonding on the prediction of pavement life, *Procees ICE-Transp* 156 (2003) 73–83.
- [6] F. Canestrari, G. Ferrotti, X. Lu, A. Millien, M.N. Partl, C. Petit, et al., Mechanical testing of interlayer bonding in asphalt pavements, advances in interlaboratory testing and evaluation of bituminous materials, Springer, 2013303–360.
- [7] M. Partl, C. Raab, Shear adhesion between top layers of fresh asphalt pavements, Switzerland, Proceedings of the 7th Conference on Asphalt Pavements for Southern Africa, Victoria Falls, 1999.
- [8] C. Tozzo, N. Fiore, A. D'Andrea, Dynamic shear tests for the evaluation of the effect of the normal load on the interface fatigue resistance, *Constr Build Mater* 61 (2014) 200–205.
- [9] M. Diakhaté, C. Petit, A. Millien, A. Phelipot-Mardel, B. Pouteau, H. Goacolou, Comparison of direct shear and torque tests for determining viscoelastic shear behaviour of tack coats, In: Proceedings of the International Conference on advanced characterization of pavement and soil engineering materials, CRC Press, Athens, Greece, 2007, pp. 281–290.
- [10] F. Canestrari, E. Santagata, Temperature effects on the shear behaviour of tack coat emulsions used in flexible pavements, *Int J Pavement Eng* 6 (2005) 39–46.
- [11] S.A. Romanoschi, J.B. Metcalf, Characterization of asphalt concrete layer interfaces, *Transport Res Record: J Transport Res Board* 1778 (2001) 132–139.
- [12] E.K. Tschegg, G. Kroyer, D.-M. Tan, S.E. Stanzl-Tschegg, J. Litzka, Investigation of bonding between asphalt layers on road construction, *J Transp Eng* 121 (1995) 309–316.
- [13] A. Zofka, M. Maliszewski, A. Bernier, R. Josen, A. Vaitkus, R. Kleizienė, Advanced shear tester for evaluation of asphalt concrete under constant normal stiffness conditions, *Road Mater Pavement Design* 16 (2015) 187–210.
- [14] S. Hakimzadeh, N.A. Kebede, W.G. Buttlar, S. Ahmed, M. Exline, Development of fracture-energy based interface bond test for asphalt concrete, *Road Mater Pavement Design* 13 (2012) 76–87.
- [15] A. Rahman, C. Ai, C. Xin, X. Gao, Y. Lu, State-of-the-art review of interface bond testing devices for pavement layers: toward the standardization procedure, *J Adhes Sci Technol* 31 (2017) 109–126.
- [16] R.C. West, J.R. Moore, J. Zhang, Evaluating tack coat applications and the bond strength between pavement layers, In: Airfield and highway pavements specialty conference ASCE Atlanta, GA, 2006, pp. 578–588.
- [17] J.-S. Chen, C.-C. Huang, Effect of surface characteristics on bonding properties of bituminous tack coat, *Transport Res Record: J Transport Res Board* 2180 (2010) 142–149.
- [18] L.N. Mohammad, M.A. Raqib, B. Huang, Influence of asphalt tack coat materials on interface shear strength, *Transport Res Record: J Transport Res Board* 1789 (2002) 56–65.
- [19] A. Collop, N. Thom, C. Sangiorgi, Assessment of bond condition using the Leutner shear test, *Procees ICE-Transport* 156 (2003) 211–217.
- [20] A. Karshenas, S.-H. Cho, A. Tayebali, M. Guddati, Y. Kim, Importance of normal confinement to shear bond failure of interface in multilayer asphalt pavements, *Transport Res Record: J Transport Res Board* (2014) 170–177.
- [21] Das R, Mohammad L.N, Elseifi M, Cao W, Cooper SB. Effects of tack coat application on interface bond strength and short-term pavement performance, *Transportation Research board 96th annual meeting*, Washington, U.S.; 2017.
- [22] X. Hu, L.F. Walubita, Effects of layer interfacial bonding conditions on the mechanistic responses in asphalt pavements, *J Transp Eng* 137 (2010) 28–36.
- [23] L.N. Mohammad, M. Hassan, N. Patel, Effects of shear bond characteristics of tack coats on pavement performance at the interface, *Transport Res Record: J Transport Res Board* 2209 (2011) 1–8.
- [24] A. D'Andrea, C. Tozzo, Interface stress state in the most common shear tests, *Constr Build Mater* 107 (2016) 341–355.
- [25] S.-H. Cho, A. Karshenas, A.A. Tayebali, M.N. Guddati, Y.R. Kim, A mechanistic approach to evaluate the potential of the debonding distress in asphalt pavements, *Int J Pavement Eng* (2016) 1–13.
- [26] M. Diakhaté, A. Phelipot, A. Millien, C. Petit, Shear fatigue behaviour of tack coats in pavements, *Road Mater Pavement Design* 7 (2006) 201–222.
- [27] M. Diakhaté, A. Millien, C. Petit, A. Phelipot-Mardel, B. Pouteau, Experimental investigation of tack coat fatigue performance: towards an improved lifetime assessment of pavement structure interfaces, *Constr Build Mater* 25 (2011) 1123–1133.
- [28] C. Tozzo, A. D'Andrea, L.L. Al-Qadi, Prediction of fatigue failure at asphalt concrete layer interface from monotonic testing, *Transport Res Record: J Transport Res Board* 2507 (2015) 50–56.
- [29] Amelian S, Kim Y.-R. Performance assessment of interlayers with different tack coats by considering loading types and failure modes, *Transport Res Record*, 0 0361198118768528.
- [30] J. Zhang, S. Wu, Z. Zhang, J. Cai, J. Chen, Failure mode and bonding evaluation at the interface between asphalt surface and semirigid base, *J Mater Civ Eng* 29 (2017) 04017100.
- [31] A.H. De Bondt, Anti-reflective cracking design of (reinforced) asphaltic overlays, Ph.D. thesis Delft University of Technology, Delft, Netherlands, 1999.
- [32] Code of China (JTG F40-2004), in: Technical specifications for construction of highway asphalt pavements, Beijing, 2004.
- [33] C. Ai, A. Rahman, F. Wang, E. Yang, Y. Qiu, Experimental study of a new modified waterproof asphalt concrete and its performance on bridge deck, *Road Mater Pavement Design* 18 (2017) 270–280.